Journal of Vertebrate Paleontology

ISSN: 0272-4634 (Print) 1937-2809 (Online) Journal homepage: www.tandfonline.com/journals/ujvp20

# Patterns of postcranial fusion in the emu (*Dromaius novaehollandiae*) and Cretaceous theropod dinosaur *Troodon formosus*

Heath R. Caldwell, Emilio Bedolla & David J. Varricchio

**To cite this article:** Heath R. Caldwell, Emilio Bedolla & David J. Varricchio (14 May 2025): Patterns of postcranial fusion in the emu (*Dromaius novaehollandiae*) and Cretaceous theropod dinosaur *Troodon formosus*, Journal of Vertebrate Paleontology, DOI: 10.1080/02724634.2025.2493166

**To link to this article:** https://doi.org/10.1080/02724634.2025.2493166

Journal of Vertebrate Paleontology e2493166 (15 pages)
Published with license by the Society of Vertebrate Paleontology.
DOI: 10.1080/02724634.2025.2493166



ARTICLE

# PATTERNS OF POSTCRANIAL FUSION IN THE EMU (*DROMAIUS NOVAEHOLLANDIAE*) AND CRETACEOUS THEROPOD DINOSAUR *TROODON FORMOSUS*

HEATH R. CALDWELL, * EMILIO BEDOLLA, and DAVID J. VARRICCHIO
Department of Earth Sciences, Montana State University, Bozeman, Montana, 59717, U.S.A., caldwellheath@outlook.com; workbedolla@gmail.com; djv@montana.edu

ABSTRACT—Skeletal fusion has been a widely used indicator of maturity for fossil vertebrate specimens, including non-avian dinosaurs. However, recent research has highlighted the potential variability in fusion patterns that can exist among closely related vertebrates. Making more justified ontogenetic interpretations for fossil specimens requires the fusion patterns of extinct and extant taxa to be assessed whenever possible. In the case of Cretaceous paravian dinosaurs, a refined understanding of postcranial fusion is lacking. Here, we describe the patterns of postcranial fusion in the extant emu (*Dromaius novaehollandiae*) and in a Cretaceous theropod *Troodon formosus*. Our results suggest similarity in fusion patterns of the postcranial axial column between the two taxa. Both taxa exhibit a bidirectional pattern of neurocentral suture closure that begins anteriorly and posteriorly before converging in the sacral region and is complete before maximum body size is obtained. This pattern contrasts with the caudocranial directionality of crocodilians and the apparent craniocaudal directionality of some neognath birds and highlights that complete neurocentral suture closure is not always an indicator of maturity. Additionally, observed fusion of the atlas, axis, cervical ribs, and sacrum/synsacrum are events that happen late in ontogeny. Appendicular fusion is an ontogenetically delayed event for both taxa as well, although it is far more extensive in the emu than in *Troodon*. These data expand upon how ontogenetic interpretations for extinct paravian dinosaurs should be made and emphasizes the diversity of fusion patterns among Archosauria.

SUPPLEMENTARY FILE(S)—Supplementary file(s) are available for this article for free at www.tandfonline.com/UJVP

Citation for this article: Caldwell, H. R., Bedolla, E., & Varricchio, D. J. (2025) Patterns of postcranial fusion in the emu (*Dromaius novaehollandiae*) and Cretaceous theropod dinosaur *Troodon formosus*. *Journal of Vertebrate Paleontology*. https://doi.org/10.1080/02724634.2025.2493166

Submitted: September 25, 2024
Revisions received: March 29, 2025
Accepted: April 3, 2025

## INTRODUCTION

Determining the relative ontogenetic stages of fossil archosaur specimens has been the subject of intensive study through a variety of approaches including morphometric (e.g., Dodson, 1975), histological (e.g., Woodward et al., 2020), and skeletal fusion analyses (e.g., Brochu, 1996). One study, Brochu (1996), describes the patterns of neurocentral suture closure in extant crocodilians as having a caudocranial directionality, with those of the cervical vertebrae being fused in only the most mature individuals. Numerous studies have used Brochu (1996) as a baseline for interpreting the ontogenetic stage of various dinosaur specimens, particularly where a complete growth series of a taxon is not known (e.g., Carrano et al., 2002; Norell et al., 2006; Smith et al., 2007; Yates & Kitching, 2003). However, the reported diversity in the pattern and timing of neurocentral suture closure among many archosaur groups, especially dinosaurs, highlights the issues of using crocodilians as an ontogenetic analogue (Brochu, 1996; Griffin, 2018; Griffin et al., 2021; Heinrich et al., 2021; Hone et al., 2016; Irmis, 2007; O'Connor, 2007; Poust et al., 2020; Stark, 1993). Other postcranial fusion features have been used as indicators of maturity, despite a lack of detailed understanding of their ontogenetic or evolutionary patterns (e.g., Longrich & Currie, 2009; Longrich & Saitta, 2024). These studies emphasize the need for more refined analyses of the patterns and timing of skeletal fusion for individual groups within Archosauria before these features can be used for ontogenetic interpretations (Griffin et al., 2021).

The ontogenetic patterns of many extinct paravian dinosaurs (those that are more closely related to crown birds than oviraptorosaurs) are especially poorly understood and convoluted (Poust et al., 2020). For instance, the seemingly immature skeletal proportions for specimens of the small troodontid *Mei long* contrast with the presence of extensive skeletal fusion and bone microstructure typically associated with maturity (Gao et al., 2012; Xu & Norell, 2004). This lack of understanding has been the source of some confusion surrounding the taxonomic status of many fossil specimens within Paraves. For example, small troodontid specimens previously suggested to be immature

*Corresponding author.


Color versions of one or more of the figures in the article can be found online at www.tandfonline.com/ujvp.

Published online 14 May 2025

individuals of *Saurornithoides mongoliensis* and *Byronosaurus jaffei* are now considered to be distinct species, which is in part based on these specimens possessing skeletal features typically associated with maturity (Bever & Norell, 2009; Currie & Peng, 1993; Pei et al., 2017; Xu et al., 2012). Understanding the precise pattern and timing of skeletal fusion events through ontogeny in paravian dinosaurs can help resolve some of the issues surrounding the interpretation of fossil specimens.

Previous research has documented dissimilarity in skeletal fusion patterns between non-avian dinosaurs, extant crocodilians, and neognath birds (Irmis, 2007). However, the lack of a growth series for many extinct archosaur taxa has prevented precise interpretations for many fossil specimens, including paravian dinosaurs (Griffin et al., 2021, Poust et al., 2020). A more informed understanding of the postcranial fusion patterns in large paravian dinosaurs can be accomplished through the analysis of extant and extinct taxa in tandem. The troodontid *Troodon formosus* is unique for being one of the larger Cretaceous paravian dinosaurs for which a relatively complete growth series is known, making it an ideal candidate for ontogenetic analysis (Varricchio, 1993; Varricchio et al., In Press). Despite the amount of material preserved for *Troodon*, the gaps in the growth series require the use of an extant analogue, such as the emu (*Dromaius novaehollandiae*). The use of the emu, as opposed to a crocodilian, as an ontogenetic analogue for a paravian such as *Troodon* is justified not only by the relatively close phylogenetic relationship (Agnolin et al., 2019), but also biomechanical similarities. Both the emu and *Troodon* exhibit similarities in skeletal growth (Castanet et al., 2000; Cubo et al., 2012; Erickson et al., 2007; Varricchio, 1993) and, unlike most neognath birds, have similar body masses and locomotor strategies as bipedal, non-volant animals (Campione et al., 2014). There is an extensive body of research (e.g., James, 2009; Gambaryan et al., 2005; Mulder, 2001; VanBuren & Evans, 2016) suggesting that similarities in skeletal fusion are related to shared biomechanical stresses. Following this assumption, even though *Troodon* is equally related to neognath and paleognath birds such as the emu, the latter is more likely to reflect the fusion patterns of *Troodon*.

Here, we describe the patterns of postcranial fusion through ontogeny in the emu and *Troodon formosus*. This analysis allows for a better understanding of the evolution of skeletal fusion in Archosauria and provides a more informed framework for interpreting the growth stages of fossil paravian specimens.

## MATERIALS AND METHODS

### Specimen Collection and Preparation

The postcranial skeletons of 12 individual emus were analyzed (Table 1). Eleven of these individuals were donated to Montana State University from a private company (Montana Emu Ranch), and one specimen was from the Montana State University Paleontology Department teaching collection (EMU-235). The donated emus were reported to have died of natural causes before being obtained for this study (Boekenheide, 2023). Emus were de-fleshed using a combination of manual maceration methods and placement in a dermestid beetle colony. Specimens were then de-greased through soaking in aqueous solutions of Tergazyme or ammonia for multiple weeks at a time. The ages for two emus (EMU-143 at 99 days and EMU-181 at 135 days) are known and were recorded by the company. The sexes of the individuals are not known. It is important to note that emus are slightly sexually dimorphic in body mass, with adult males reported to have a maximum body mass about 90% of adult females (Maloney & Dawson, 1993).

The sample of *Troodon formosus* specimens evaluated consists of three associated skeletons (MOR 430, 563, 748) and the remains of multiple individuals from a bonebed (MOR 553) (Varricchio, 1995) (Table 2). We follow the justification of Varricchio et al. (2018, In Press) for using the name *Troodon formosus* for this taxon, as defined by Currie (1987). All specimens were collected from the Two Medicine Formation of Montana (Varricchio et al., In Press).

TABLE 1. Measured femur lengths (millimeters) and ages (days) for emu specimens used in this study. '*' indicates estimated femur length. '**' indicates estimated ages. '***' indicates estimated ages based on the extrapolation of data.

| Specimen | Femur Length (mm) | % Maximum Femur Length | Age (Days) |
|---|---|---|---|
| EMU-45 | 45 | 19 | 9** |
| EMU-63 | 63 | 27 | 26** |
| EMU-143 | 143 | 61 | 99 |
| EMU-170 | 170 | 72 | 126** |
| EMU-175 | 175 | 74 | 131** |
| EMU-176 | 176* | 75 | 132** |
| EMU-181 | 181 | 77 | 135 |
| EMU-182 | 182 | 77 | 138** |
| EMU-177 | 177 | 75 | 132** |
| EMU-185 | 185 | 79 | 140** |
| EMU-209 | 209 | 89 | 162*** |
| EMU-235 | 235 | 100 | 187*** |

TABLE 2. Femur length (millimeters) and estimated age (years) values for specimens of *Troodon* based on histological analysis. '*' indicates a locality for which multiple *Troodon* individuals were collected.

| Specimen | Femur Length (mm) | % Maximum Femur Length | Estimated Age |
|---|---|---|---|
| MOR 430 | 126 | 39 | < 1 year |
| MOR 553* | 218-330 | ~70–100 | ~2–9 years |
| MOR 563 | 220 | ~70 | ~1 year |
| MOR 748 | 320 | 100 | ~9-18 years |

### Ontogenetic Stage Determination

Although the ages of only 2 out of the 12 emus are known in this dataset, we follow the assumptions of Goonewardene et al. (2003) that individual size is roughly positively correlated with ontogenetic stage for this taxon. Femur length was used as an approximation for relative ontogenetic stage based on the assumption that emus with a greater body size are more skeletally mature (Campione et al., 2014; Goonewardene et al., 2003). This assumption is supported by the fact that all these individuals were raised in captivity. Additionally, all but one of the emu specimens (EMU-235) were raised in the same facility under similar conditions. Finally, data on other emu hindlimb specimens collected from this facility show a strong positive linear relationship between femur length and emu age ($R^2 = 0.97$) (Boekenheide, 2023) (Fig. 1).

For *Troodon*, maturity of some of the specimens was assessed through histological analysis of limb bones (Boekenhide, 2023; Erickson et al., 2007; Varricchio, 1993) (Table 2). MOR 748, the largest individual in the dataset, is associated with a clutch of eggs and suggests that individuals of this approximate size were near skeletal maturity (Erickson et al., 2007; Varricchio et al., 1997, 2008). For disarticulated specimens from MOR 553, it is assumed that larger elements are from older individuals, which is corroborated by the histological analysis of disarticulated limb bones from the locality (Boekenhide, 2023; Varricchio, 1993).

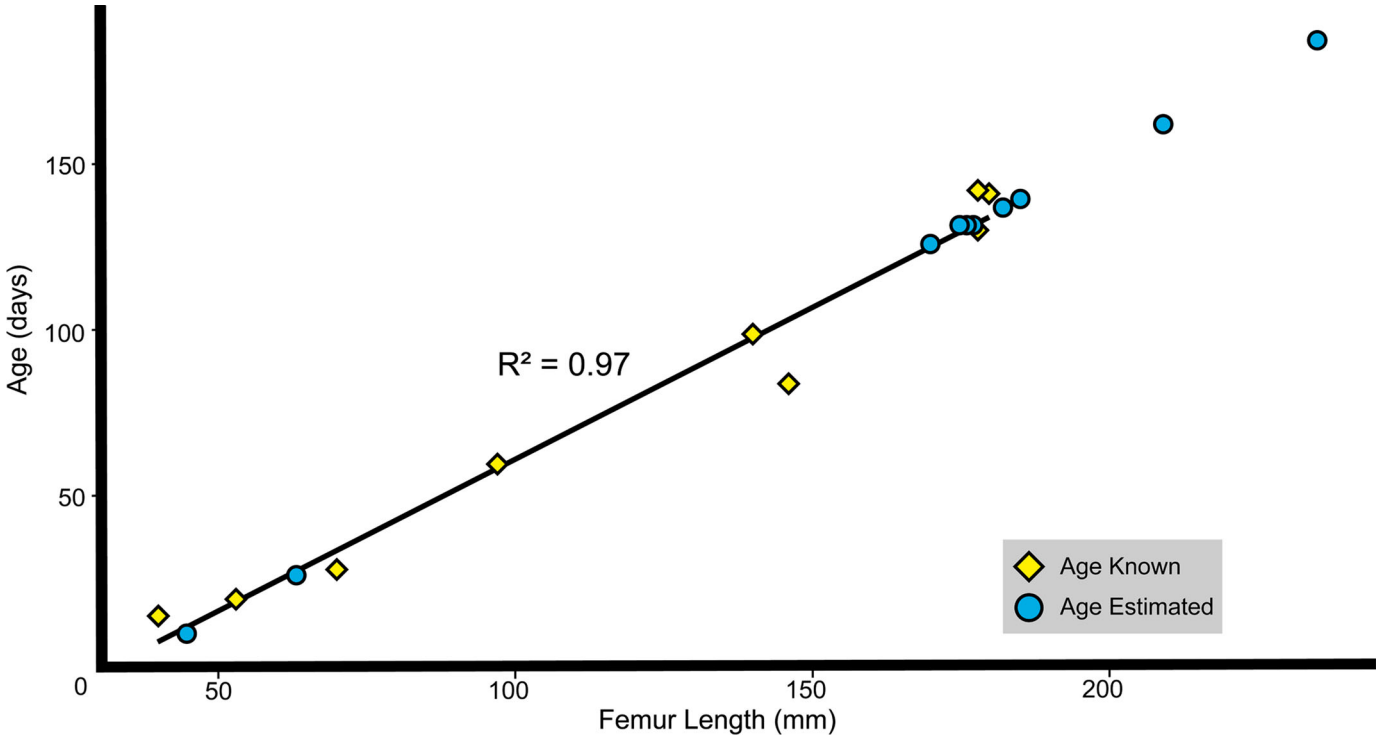


FIGURE 1. Plot of femur length against age for emu specimens. Linear regression is based on specimens of known ages (rhombus). All of these specimens were collected from the same facility with the exception of the largest individual (EMU-235). Specimens denoted by a circle have age values estimated from the linear regression. Most of the aged specimens were not included in the remainder of this study, as they lacked most of the skeleton.

### Ontogenetic Analysis

An ontogenetic analysis of fusion patterns was conducted following the methods of Brochu (1996) to more easily interpret the collected data. An ontogenetic matrix was built with Mesquite version 3.81 using skeletal fusion data in the emu postcranial skeleton. A maximum parsimony analysis with an implicit enumeration search was conducted using Tree analysis using New Technology (TNT) version 1.6 (Goloboff & Morales, 2023). This analysis included 13 operational ontogenetic units (12 emu specimens, 1 hypothetical outgroup) and 141 equally weighted ordered characters that were observed to vary in the sample (Table 3, Supplementary File 1). A hypothetical outgroup was designated with all characters coded as open (0), reflecting the assumed embryonic stage where no fusion has occurred (Brochu, 1996). Fusion state classification follows those outlined by Brochu (1996) (Fig. 2). A fully closed suture (coded as 2) is one where the suture is no longer visible. An open suture (coded as 0) is defined as having an unbroken line between the two components. A partially closed suture (coded as 1) is one where fusion has begun to occur, but the suture is still visible. Although a purely surficial examination of the sutures does not account for the subsurface patterns of fusion, this analysis is more appropriate from a paleontological perspective, where histological or computed tomography analysis of a specimen may not be readily available to the researcher (Bailleul et al., 2016).

The characters of interest and methods used for the *Troodon* dataset are the same as those used for the emu dataset with the added character of fusion of the astragalus to the calcaneum (Table 3, Supplementary File 2). Given the more incomplete *Troodon* sample, specimens belonging to individuals of similar body sizes were grouped together into singular operational ontogenetic units and characters from the same body region (e.g., dorsal vertebrae, caudal vertebrae) were grouped together. The

TABLE 3. An abbreviated list of the characters used in ontogenetic analysis of the emu and *Troodon* growth series.

| Skeletal Region | Characters |
|---|---|
| Atlas (1st Cervical Vertebra) | Fusion of the right and left lateral processes of the vertebral arch to each other and to the atlantal intercentrum. |
| Axis (2nd Cervical Vertebra) | Fusion of the axial intercentrum and the atlantal pleurocentrum to the axial pleurocentrum. |
| 3rd – 18th Cervical Vertebra | Fusion of the cervical ribs to the parapophyses and diapophyses of the cervical vertebrae. |
| 2nd Cervical Vertebra–20th Sacral Vertebra | Closure of the neurocentral suture. |
| 9th Dorsal–20th Sacral Vertebra | Fusion of the neural spines and centra in the synsacrum to their respective elements in the adjacent vertebrae. |
| Sacral Ribs | Fusion of sacral ribs to synsacrum |
| Synsacrum | Fusion of the 9$^{th}$ dorsal and sacral vertebrae to the ilia. |
| Pectoral Girdle | Fusion of the scapula to the coracoid. |
| Sternum | Fusion of the left and right components of the sternum. |
| Metatarsus | Fusion of the metatarsals to each other. |
| Tarsometatarsus | Fusion of the tarsus to the metatarsus. |
| Acetabulum | Fusion of the pubis to ilium, ischium to ilium, and ischium to pubis. |
| Posterior Pelvis | Fusion of the ischial boot to the distal ilium. |
| Tibiotarsus | Fusion of the proximal epiphysis and astragalus to the tibiotarsus. |
| Astragalus and Calcaneum | Fusion of the astragalus to the calcaneum (*Troodon* only). |

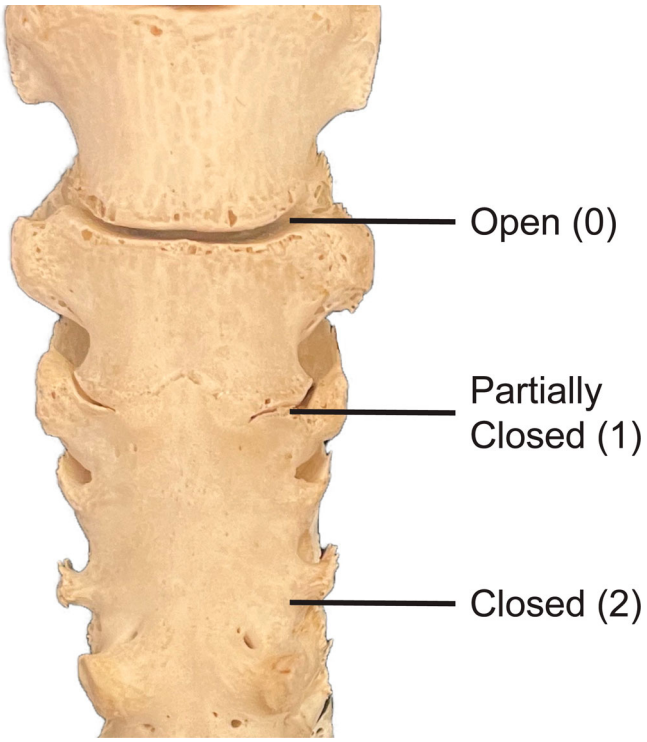


FIGURE 2. Partial synsacrum of EMU-177 in ventral view with examples of how skeletal fusion was categorized. Not to scale.

character matrix for *Troodon* consists of 5 operational ontogenetic units (4 body-size categories, 1 hypothetical outgroup) and 6 equally weighted ordered characters (Supplementary File 3). The degree of skeletal fusion for each specimen was noted and compared with the more complete emu growth series.

**Institutional Abbreviations**—**MOR**, Museum of the Rockies, Bozeman, Montana, U.S.A.

## RESULTS

### Ontogenetic Analysis

A single most parsimonious tree was recovered for both the emu and *Troodon* analyses (Fig. 3, Supplementary File 2, Supplementary File 4). In both cases, specimens generally grouped together sequentially by femur length with the exception of a 'sister taxa' relationship that was recovered between EMU-177 (75% mfl) and EMU-182 (77% mfl).

### Emu

**Axial Skeleton**—Fusion of the atlas is complete only for the largest individual in the dataset at 100% maximum femur length (mfl) (EMU-235) (Fig. 4). At about 89% mfl (EMU-209), the lateral processes of the atlas are fused to the atlantal intercentrum, but not to each other. No fusion has occurred in the atlas for the next largest individual in the dataset, EMU-185 (79% mfl) (Fig. 4).

For the axis, an open neurocentral suture is present in the smallest individual (EMU-45, 19% mfl), but is closed for all larger individuals in the sample (Fig. 5). Partial fusion of the atlantal pleurocentrum to the axial pleurocentrum is present in EMU-143 (61% mfl) and is complete by the growth stage of EMU-209 (89% mfl). However, there are individuals of sizes intermediate between EMU-143 and EMU-209 for which this feature is not fused. Fusion of the axial intercentrum to the axial pleurocentrum begins by the growth stage of EMU-181 (77% mfl) and is only fully fused by the growth stage of EMU-209 (89% mfl).

No open neurocentral sutures in the cervical vertebrae (excluding the atlas and axis) were observed for the specimens in this dataset, including the smallest individual, EMU-45, at 19% mfl (Fig. 6). Fusion of the cervical ribs to the diapophyses

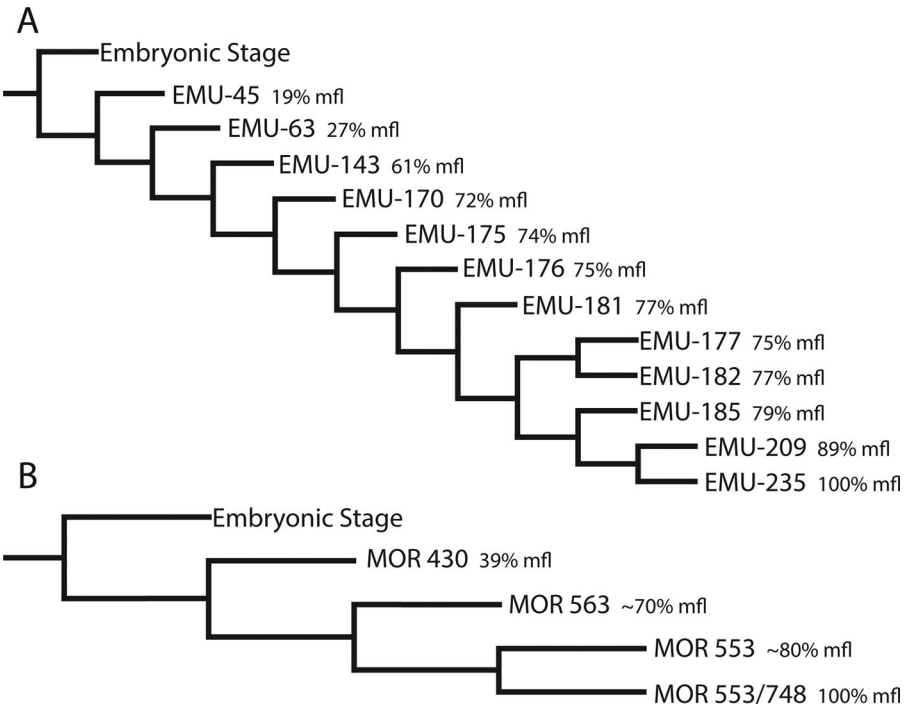


FIGURE 3. Most parsimonious trees resolved from the ontogenetic analyses. **A**, emu data set; **B**, *Troodon* data set. **Abbreviation**: **mfl**, maximum femur length.

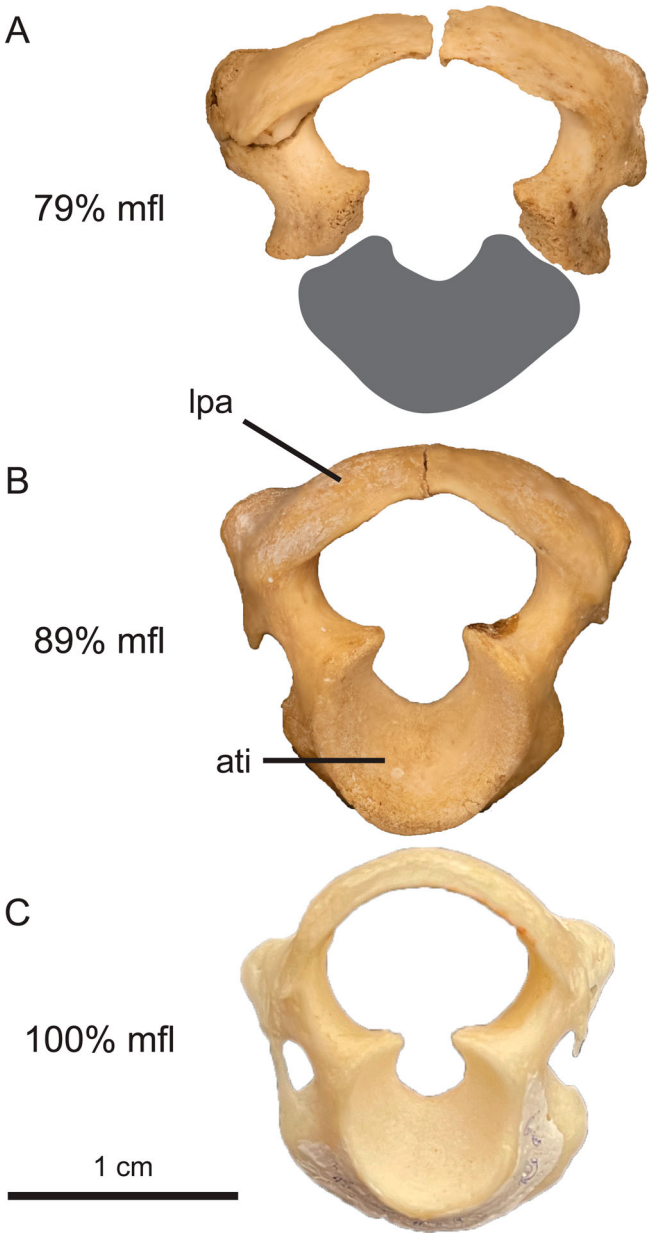


FIGURE 4. Emu atlases in anterior view. **A**, EMU-185; **B**, EMU-209; **C**, EMU-235. **Abbreviations**: **ati**, atlantal intercentrum; **lpa**, lateral process of atlas; **mfl**, maximum femur length. Gray silhouette corresponds to atlantal intercentrum lost during preparation.

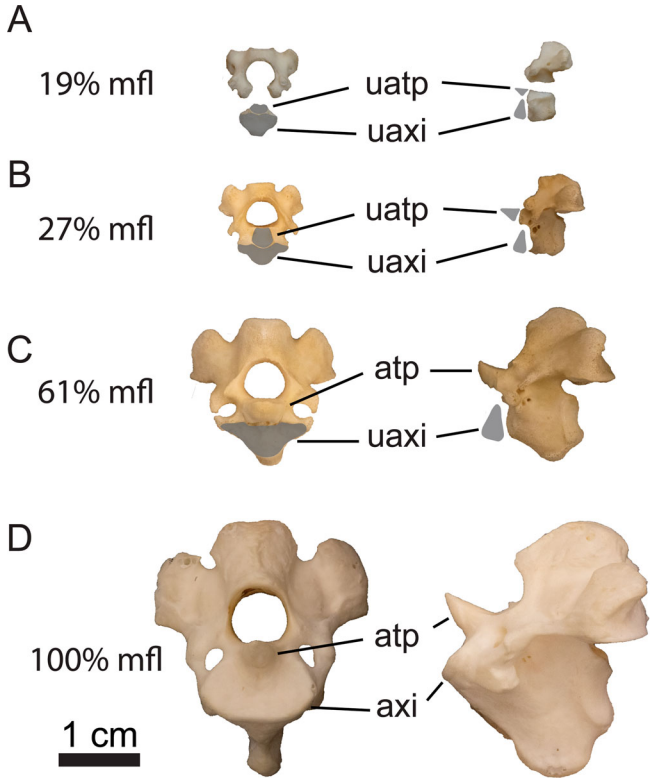


FIGURE 5. Emu axes in anterior (left) and left lateral (right) views. **A**, EMU-45; **B**, EMU-63; **C**, EMU-143; **D**, EMU-235. **Abbreviations**: **atp**, atlantal pleurocentrum; **axi**, axial intercentrum; **mfl**, maximum femur length; **uatp**, unfused atlantal pleurocentrum; **uaxi**, unfused axial intercentrum. Gray silhouettes correspond to elements lost during preparation.

is complete by the growth stage of EMU-209 (89% mfl) for all cervical ribs (Fig. 7A). Fusion between the cervical ribs and parapophyses in EMU-209 (89% mfl) is complete for all cervical vertebrae except the posterior-most one, where the suture is open. Fusion of the cervical ribs to the parapophyses and diapophyses is complete in only the largest individual of the dataset, EMU-235 (100% mfl). By contrast, EMU-185 (79% mfl) and the smaller individuals present no fusion of cervical rib features.

Neurocentral sutures of the dorsal vertebrae are completely closed for emus by the growth stage of EMU-143 (61% mfl) (Fig. 6). For EMU-45 (19% mfl) and EMU-63 (27% mfl), the posterior dorsal vertebrae have partially open neurocentral sutures, while those more anterior are fully closed.

For the synsacrum, neurocentral suture closure begins by the growth stage of EMU-63 (27% mfl) and is complete by the growth stage of EMU-185 (79% mfl) (Fig. 6). The last neurocentral sutures to close are those adjacent to the acetabulum. Neurocentral sutures anterior and posterior to the acetabulum are mostly closed by the growth stage of EMU-143 (61% mfl). Fusion of the sacral ribs to the centra is complete by ontogenetic stage of EMU-185 (79% mfl) but begins by the growth stage of EMU-63 (27% mfl) (Fig. 8). Fusion of adjacent sacral vertebrae to one another begins by the ontogenetic stage of EMU-143 (61% mfl) but is only complete in EMU-235 (100% mfl) (Fig. 9). Vertebral fusion begins near the region of the acetabulum before progressing anteriorly and posteriorly. The sutures between partially fused sacral centra are notably more sinuous than the approximately linear sutures of other elements. Fusion of the synsacrum to the ilia begins by the growth stage of EMU-209 (89% mfl) and is complete in EMU-235 (100% mfl). In EMU-209, all but the anterior and posterior-most vertebrae of the synsacrum are fully fused to the ilia.

Neurocentral sutures in the caudal vertebrae are fully closed by the growth stage of EMU-45 (19% mfl) (Fig. 6). The absolute timing of the fusion of the pygostyle cannot be determined, as this element was lost during the preparation of the skeletons for many individuals.

**Appendicular Skeleton**—The sternum is unfused in EMU-63 (27% mfl) but is fully fused in EMU-143 (61% mfl) (Fig. 10). The ischium fuses to the pubis by the growth stage of EMU-185 (79% mfl) before the two elements fuse to the ilium, forming the margin of the acetabulum by the growth stage of EMU-209 (89% mfl). Fusion of the scapulocoracoid, and astragalus to tibia is also complete by the growth stage of EMU-209

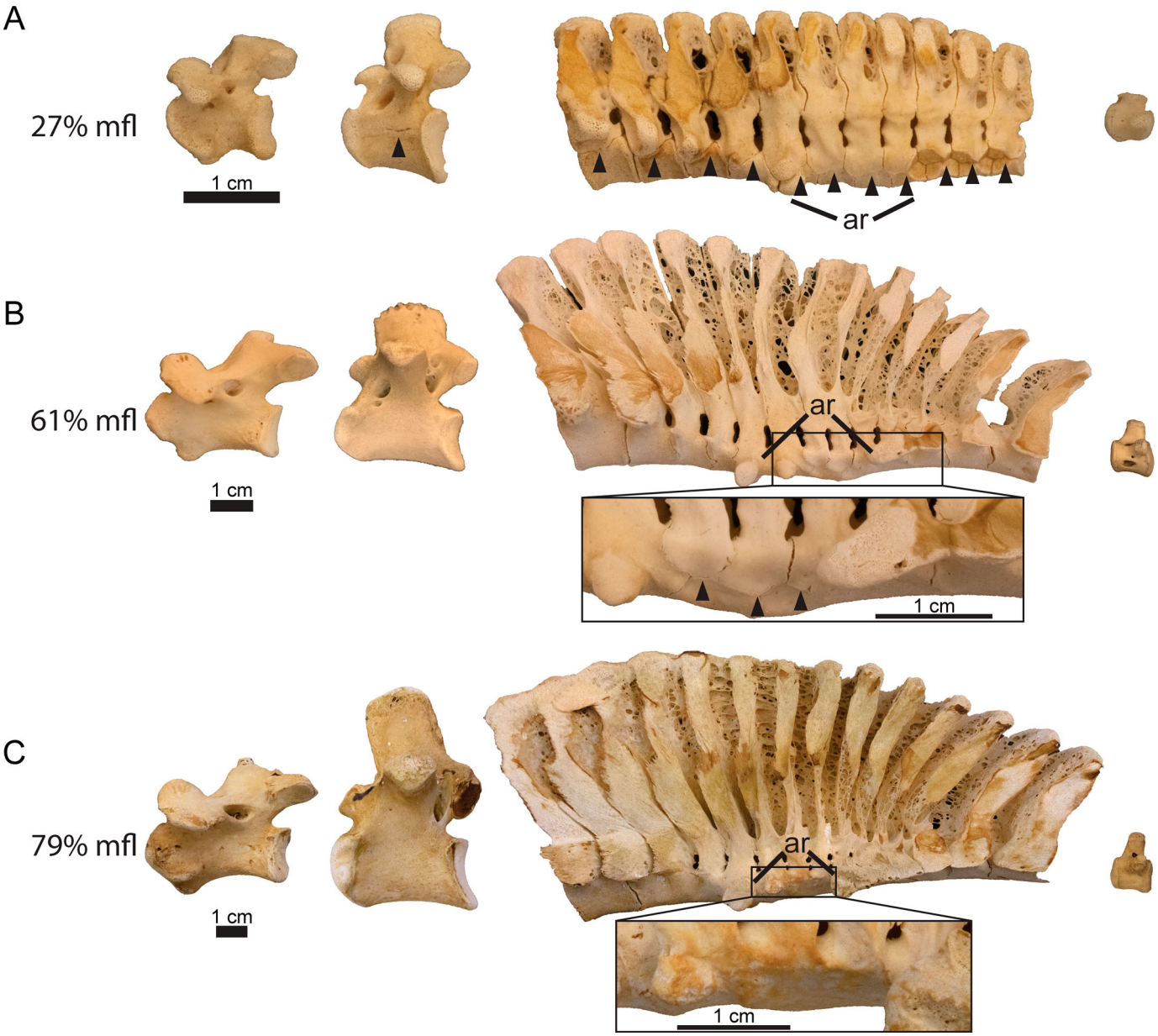


FIGURE 6. From left to right, posterior cervical vertebrae, posterior dorsal vertebrae, partial synsacra, and caudal vertebrae from the emu in left lateral view. **A**, EMU-63; **B**, EMU-143; **C**, EMU-185; **Abbreviations**: **ar**, acetabular region; **mfl**, maximum femur length. Black triangles correspond to open or partially closed neurocentral sutures.

(89% mfl). Finally, fusion of the tarsus to the metatarsus, cranial cnemial crest to the tibiotarsus, and posterior ischium and ilium occurs between the ontogenetic stages of EMU-209 and EMU-235 (89–100% mfl). Individual metatarsals within the metatarsus are partially fused to each other for all specimens in this dataset, but the proximal fusion of these elements is only complete in EMU-235 (100% mfl).

### Troodon

**Axial Skeleton**—Apart from the atlas, all preserved cervical vertebrae possess fully closed neurocentral sutures, with the smallest individual being MOR 430 (39% mfl) (Fig. 11). However, open neurocentral sutures for the cervical vertebrae are present in embryonic remains of *Troodon* (MOR 246) (Varricchio et al., 2002). MOR 563 (~70% mfl) possesses an unfused atlas, but no other examples of this element are preserved. Whereas large cervical vertebrae (~70–80% mfl) from MOR 553 lack fused cervical ribs, even larger specimens (~90–100% mfl) from the same locality possess fused cervical ribs (Fig. 7B).

Neurocentral sutures of the preserved dorsal vertebrae are open in MOR 430 (39% mfl) but are closed in all larger specimens (~70–100% mfl) (Fig. 11). Open neurocentral sutures in the sacral vertebrae are present in MOR 430 (~39% mfl), MOR 563 (~70% mfl), and a single specimen from MOR 553 (~70% mfl) but are closed in larger specimens from MOR 553 (~80–100% mfl) (Fig. 11). The sacrum itself is unfused in MOR 430, MOR 563, and smaller specimens of MOR 553 (~70–80% mfl). However, fully fused sacra from MOR 748 (100% mfl)

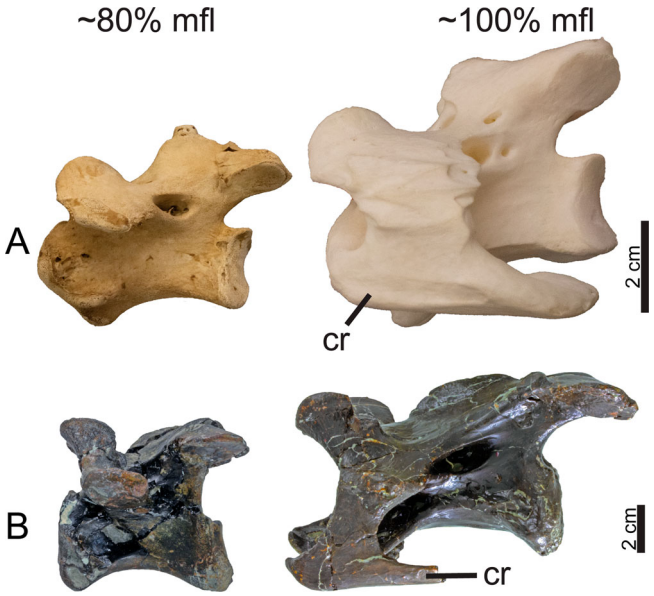


FIGURE 7. **A**, posterior cervical vertebrae from the emu and **B**, *Troodon* in left lateral view. **A**, EMU-185 (left) and EMU 235 (right); **B**, MOR 553s 7-13-91-52 (left) and MOR 553s 7-21-92-46. **Abbreviations**: **cr**, cervical rib; **mfl**, maximum femur length.

and a large individual from MOR 553 (~90–100% mfl) are preserved (Fig. 12).

The posterior caudal vertebrae (those lacking a neural spine) have closed neurocentral sutures for all specimens preserved (39–100% mfl) (Fig. 11). An anterior caudal vertebra in MOR 430 (39% mfl) possesses a partially closed neurocentral suture. All other anterior caudal vertebrae have fully closed neurocentral sutures.

**Appendicular Skeleton**—For the characters of interest, the only definitive appendicular fusion in *Troodon* is between the astragalus and the calcaneum from MOR 748 (100% mfl) and large specimens from MOR 553 (astragalus lateral condyle height between 27.8 and 32.3 mm) (Fig. 13). Smaller astragali from MOR 553 and MOR 430 (astragalus lateral condyle height between 10.7 and 19.9 mm) are not fused to a calcaneum. There is possible fusion of the right tarsometatarsus in MOR 748, although the left tarsometatarsus is clearly unfused in this individual. Preserved pelvic elements from MOR 553 (pubis length: ~220 mm, ischium length: ~200 mm) show no signs of fusion. However, fused pelvic elements are known in other large troodontid specimens of the region (van der Reese & Currie, 2017).

## DISCUSSION

### Ontogenetic Analysis

The ontogenetic analyses of the emu and *Troodon* both recovered single most parsimonious trees that generally group specimens sequentially by femur length. These results are likely reflecting the low amount of ontogenetic sequence polymorphism for these taxa, which aligns with what has been reported for other crown birds and closely related theropods (Griffin & Nesbitt, 2016). The single instance of a 'sister-taxa' relationship in the emu growth series reflects some variation in the ontogenetic sequence of postcranial fusion for this taxon (Griffin & Nesbitt, 2016). It is also worth noting that EMU-177 possesses a pathological metatarsus. This may have stunted its growth and is potentially why it was resolved with larger individuals. These results support claims that more extensive skeletal fusion generally correlates with maturity (e.g., Griffin, 2018).

### Neurocentral Suture Closure

For the emu and *Troodon*, neurocentral suture closure is bidirectional, beginning anteriorly in the cervical vertebrae and posteriorly in the caudal vertebrae before converging on the synsacrum/sacrum later in ontogeny (Fig. 14). This contrasts with the caudocranial directionality reported for crocodilians and the purely craniocaudal condition for some neognath birds and rhynchosaurs (Brochu, 1996; Heinrich et al., 2021; Stark, 1993; Verrière et al., 2022). The bidirectional pattern of suture closure appears to be consistent with what is reported for other theropods such as dromaeosaurids (Poust et al., 2020; Wang & Pei, 2024), allosaurids (Malafaia et al., 2017), abelisaurids (O'Connor, 2007), tyrannosauroids (Nesbitt et al., 2019), and coelophysoids (Griffin, 2018). However, other theropod groups may have different patterns (Griffin et al., 2021; Irmis, 2007; Verrière et al., 2022). This includes oviraptorosaurs (Funston, 2024), which appear to have the caudocranial pattern of neurocentral suture closure observed in crocodilians.

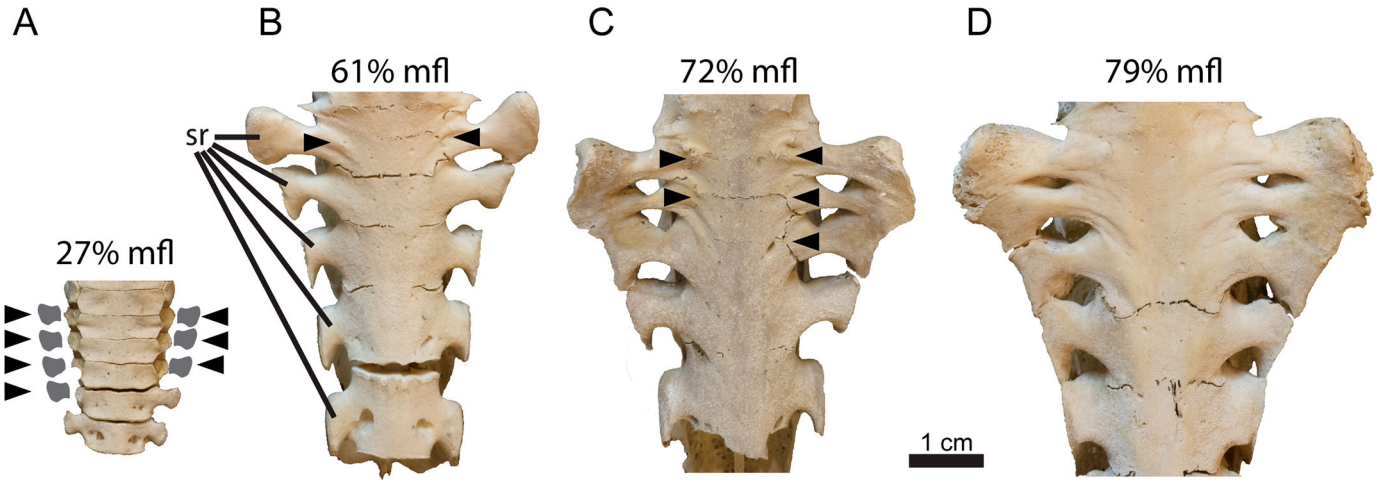


FIGURE 8. Partial emu synsacra in ventral view. **A**, EMU-63; **B**, EMU-143; **C**, EMU-170; **D**, EMU-185. **Abbreviations**: **mfl**, maximum femur length; **sr**, sacral rib. Black triangles correspond to open or partially closed sacral rib–vertebra sutures. Gray silhouettes correspond to elements lost during preparation.

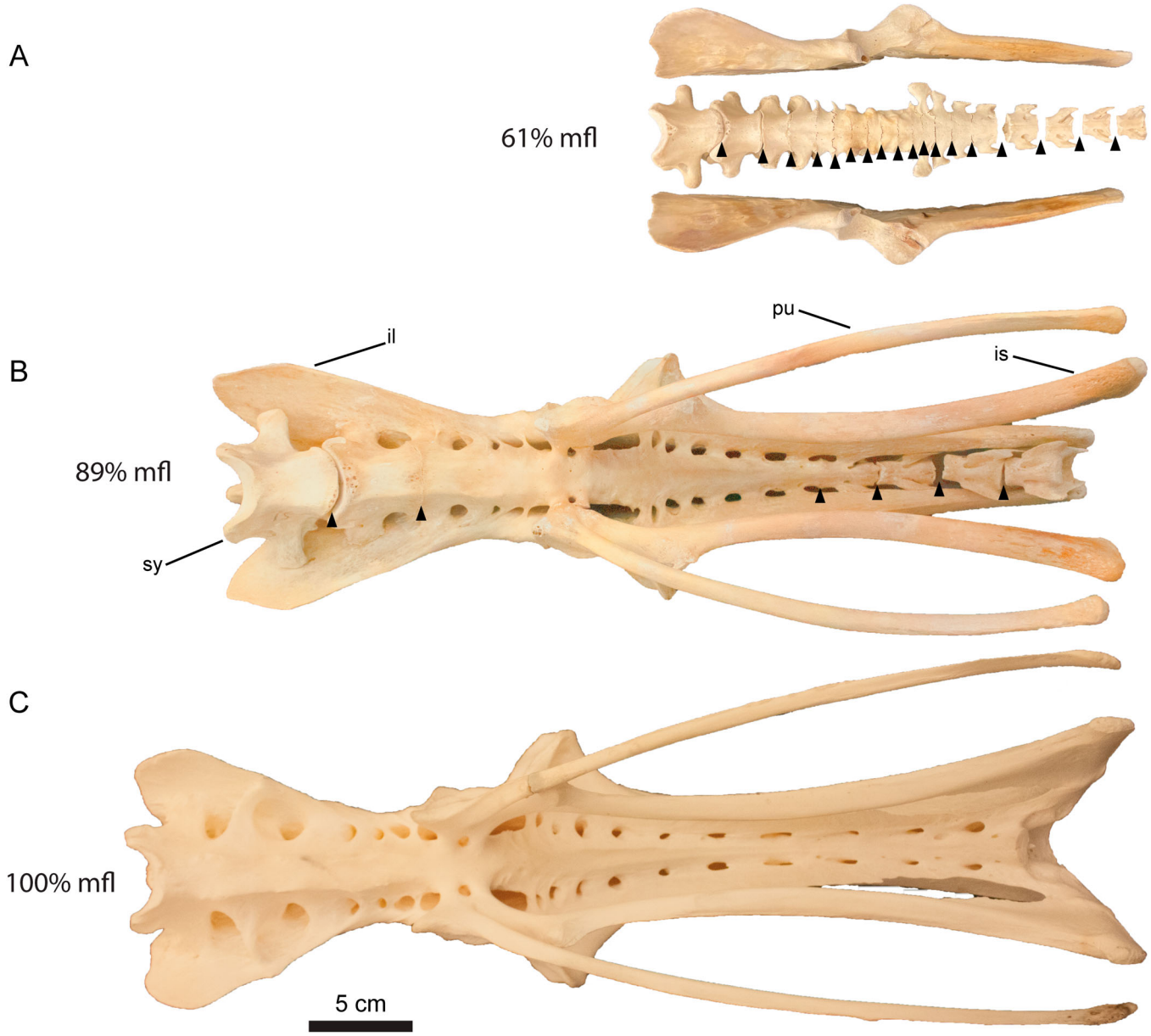


FIGURE 9. Emu pelvic girdles in ventral view. **A**, EMU-143; **B**, EMU-209; **C**, EMU-235. **Abbreviations**: **il**, ilium; **is**, ischium; **mfl**, maximum femur length; **pu**, pubis; **sy**, synsacrum. Black triangles correspond to open or partially closed sacral vertebra–vertebra sutures.

Non-atlantal neurocentral suture closure is complete for emus and *Troodon* before maximum body size is reached (~80% mfl), as is reported for most similarly sized specimens of the early theropods *Coelophysis bauri* and *Megapnosaurus rhodesiensis* (Griffin, 2018, 2021) as well as precocial neognath birds (Stark, 1993). This contrasts with extant crocodilians where only the most mature individuals exhibit complete closure of all neurocentral sutures (Brochu, 1996). The early closure of most neurocentral sutures, especially those of the non-sacral vertebrae, for both taxa in this study highlights the need for caution when using this feature as an indicator of maturity for groups where an ontogenetic series is poorly understood. Complete neurocentral suture closure has been used as the primary justification for interpretations of maturity for many maniraptoran specimens (Naish & Sweetman, 2011; Norell et al., 2009; Senter et al., 2012; Sues, 1997; Wang et al., 2022; Xu & Xiaolin, 2004). Interestingly, the closure of neurocentral sutures in the holotype specimen of the small Early Cretaceous dromaeosaurid *Yurgovuchia doellingi* was used as support for this taxon being distinct from the larger sympatric dromaeosaurid *Utahraptor ostrommaysorum*, but this does not necessarily mean these two taxa are synonymous (Senter et al., 2012). It is important to emphasize that the timing of neurocentral suture closure can be highly variable, even within restricted groups. Within Alvarezsauridae, for example, the relative timing of neurocentral suture closure has been suggested to correlate with the maximum body size specific taxa attained (Averianov et al., 2023). Given the extreme variability of body sizes among theropods and within specific theropod groups, caution is needed when applying the trends in fusion of one taxon for making interpretations of another, even

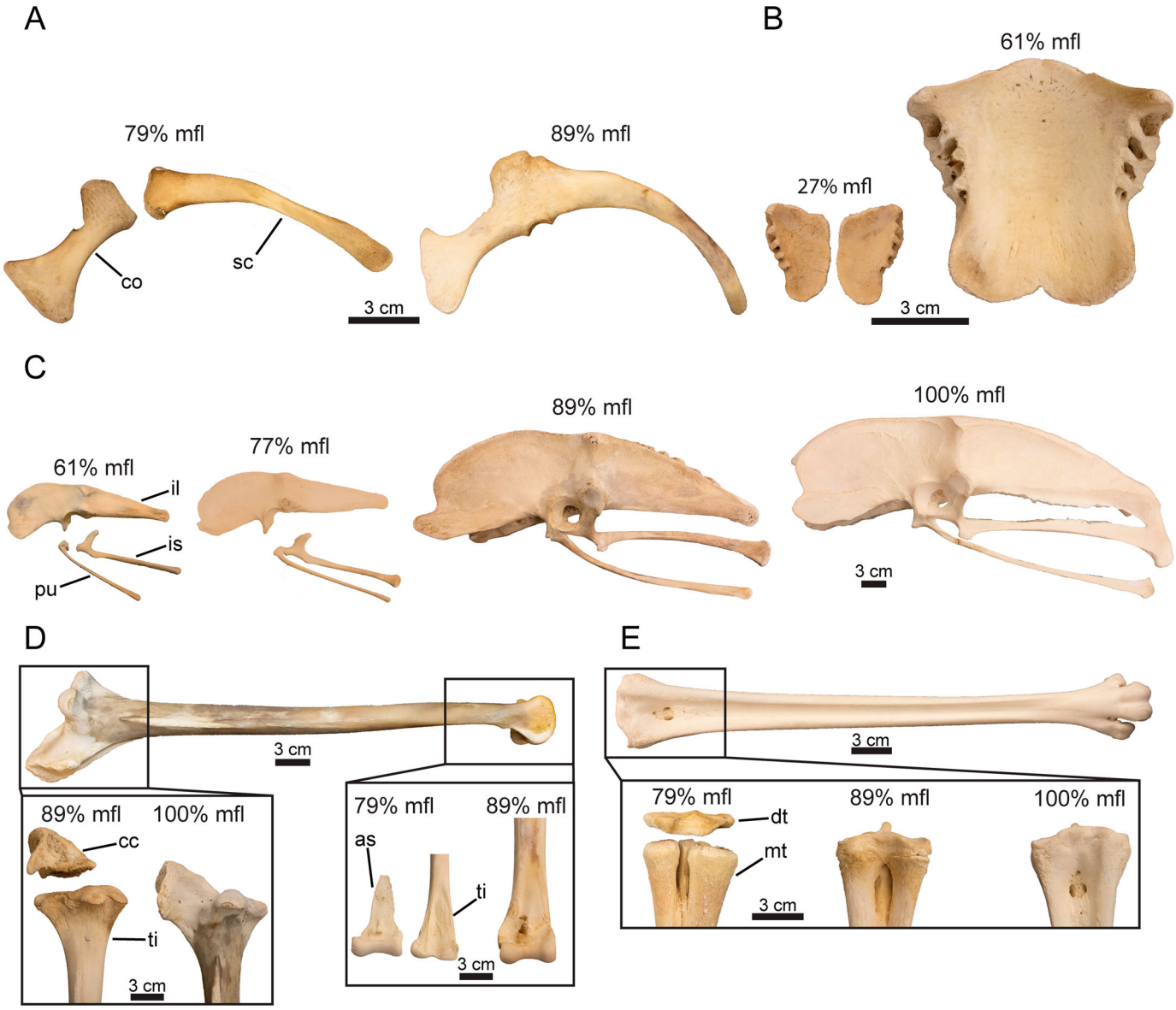


FIGURE 10. Emu appendicular elements. **A**, scapulocoracoids in left lateral view of EMU-185 (left) and EMU-209 (right); **B,** sternums in dorsal view from EMU-63 (left) and EMU-143(right); **C**, pelves in left lateral view of (from left to right) EMU-143, EMU-181, EMU-209, and EMU-235; **D**, proximal tibiotarsi of EMU-209 and EMU-235 in left lateral view, and distal tibiotarsi of EMU-185 and EMU-209 in anterior view; **E**, proximal tarsometatarsi (from left to right) of EMU-185, EMU-209, and EMU-235 in anterior view. **Abbreviations**: **as**, astragalus; **cc**, cranial cnemial crest; **co**, coracoid; **dt**, distal tarsus; **il**, ilium; **is**, ischium; **mfl**, maximum femur length; **mt**, metatarsus; **pu**, pubis; **sc**, scapula; **ti**, tibia.

if the taxa are closely related (D'Emic et al., 2023). It is possible, however, that the similarities in neurocentral suture closure for the emu and *Troodon* reflect a pattern shared among similarly sized paravians.

### Atlas and Axis Fusion

Complete fusion of the atlas occurs relatively late in ontogeny for the emu with only the largest individuals (EMU-209, EMU-235) having a fully fused atlas. An unfused atlas is preserved for MOR 563 (~70% mfl), but a lack of specimens at later growth stages prevents an assessment of when this element fuses for *Troodon*. An unfused atlas is reported for the holotype of *Dilophosaurus wetherilli* (Marsh & Rowe, 2020), a juvenile specimen of the therizinosaur *Falcarius utahensis* (Zanno, 2010), and the relatively large holotype specimen of the troodontid *Gobivenator mongoliensis* (Tsuihiji et al., 2014). Fusion of the atlas late in ontogeny also occurs in extant crocodilians (Brochu, 1996). The seemingly widespread similarity in timing of atlantal fusion across Archosauria potentially suggests that a fused atlas is a reliable indicator of skeletal maturity for members of this clade.

Similar to the atlas, fusion of the axis is complete late in ontogeny for the emu. Neurocentral suture closure for this element is complete by the growth stage of EMU-63 (27% mfl). This is then followed by fusion of the atlantal and axial pleurocentra by the growth stage of EMU-143 (61% mfl), although there are larger individuals in the dataset for which this feature is not fused. Fusion of the axial intercentrum and pleurocentrum is only complete by the growth stage of EMU-209 (89% mfl). MOR 563 (~70% mfl) possesses the only axis for the *Troodon* sample.


FIGURE 11. From left to right, posterior cervical vertebrae, posterior dorsal vertebrae, partial sacral vertebrae, anterior and posterior caudal vertebrae from *Troodon* in left lateral view, except for the cervical vertebra for MOR 430, which is in posterior view. **A**, MOR 430; **B**, MOR 563; **C**, MOR 553s; **Abbreviations**: **c**, centrum; **mfl**, maximum femur length; **na**, neural arch. Light gray triangles correspond to open or partially closed neurocentral sutures. Question mark and dark gray silhouettes correspond to material that is not preserved.

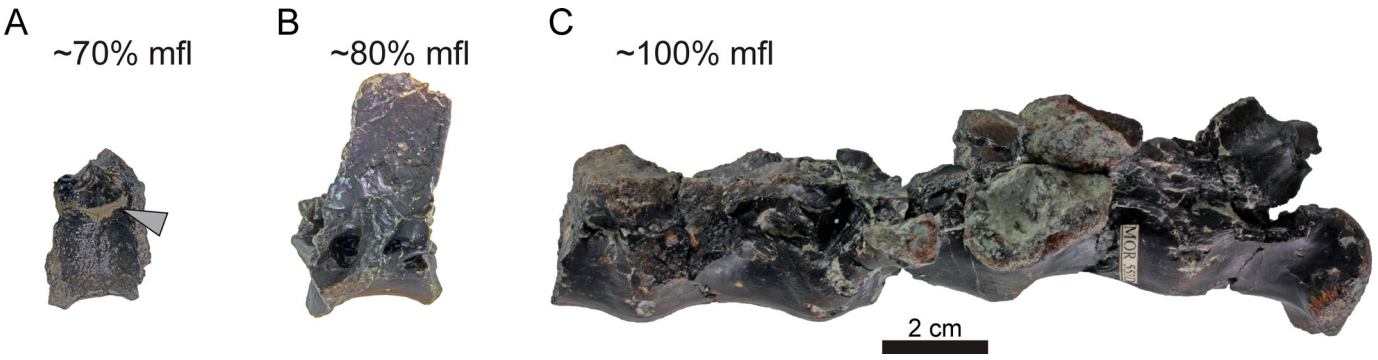


FIGURE 12. Sacral vertebrae from *Troodon* in left lateral view. **A**, MOR 563; **B**, MOR 553s 8-20-92-312; **C**, MOR 553d 02-11. **Abbreviation**: **mfl**, maximum femur length. Gray triangle corresponds to open neurocentral suture.

While the neurocentral suture is closed, poor preservation prevents an assessment of any other fusion features. A fully fused axis is present in the holotype specimens for *Yurgovuchia doellingi* (Senter et al., 2012) and *Gobivenator mongoliensis* (Tsuihiji et al., 2014). A lack of fusion between the atlantal pleurocentrum, axial pleurocentrum, and axial intercentrum is

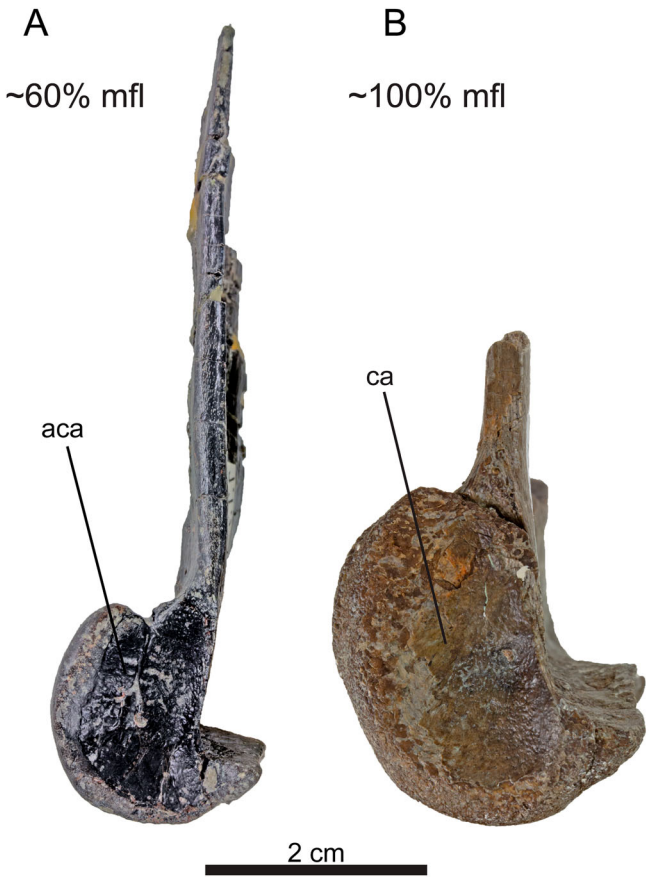


FIGURE 13. *Troodon* astragali in left lateral view. **A**, MOR 553s 7-7-91-19 (reversed); **B**, MOR 553 11-1-01-1. **Abbreviations**: **aca**, absent calcaneum; **ca**, calcaneum; **mfl**, maximum femur length.

reported for the *Dilophosaurus wetherilli* holotype specimen (Marsh & Rowe, 2020). Ontogenetically delayed fusion of these axial elements is also reported for extant crocodilians (Brochu, 1996). Like the atlas, the similarities in the timing of fusion events for the axis across Archosauria supports its use as a reliable indicator of maturity for this clade.

### Cervical Ribs

Fusion of the cervical ribs to the corresponding cervical vertebrae occurs late in ontogeny for both the emu and *Troodon*, with only the largest specimens for both taxa having fusion of the cervical ribs. At least for the emus, cervical ribs fuse to the diapophyses before fusing to the parapophyses. The incomplete cervical rib fusion for the posterior-most cervical vertebra in EMU-209 (89% mfl) contrasts with the complete fusion in the more anterior vertebrae and suggests a craniocaudal directionality of cervical rib fusion, at least for emus. Ontogenetically delayed cervical rib fusion has been suggested to be a synapomorphy for Maniraptora (Gauthier, 1986).

### Sacral Fusion

For both emus and *Troodon*, complete fusion of synsacrum/sacrum is complete for only the largest individuals (~90–100% mfl) in the dataset and is preceded by complete neurocentral suture closure. Fusion of the synsacral vertebrae for the emu begins before neurocentral suture closure is complete, unlike *Troodon*. For the emu, fusion of adjacent synsacral vertebrae appears to begin near the acetabulum, before terminating with fusion of the anterior and posterior-most vertebrae in the synsacrum. Although fusion of the sacrum appears to be a reliable indicator of maturity for paravian dinosaurs, the variability and convergence of sacrum fusion among Archosauria makes it difficult to assess how useful this character is in a broader context using the data of this study alone (Moro et al., 2021). An embryonic oviraptorosaur specimen, for example, is reported to possess sacral centra that are fully fused to each other (Norell et al., 2001). The relatively sinuous intervertebral sutures in the emu synsacrum compared with those of the rest of the postcrania is potentially reflective of the greater skeletal stress in that region (Herring, 2008).

### Appendicular Fusion

Fusion events of the appendicular skeleton are characterized by occurring relatively late in ontogeny for the emu and *Troodon*, although it is far less extensive in the latter. For the emu, all appendicular fusion events occur between the growth stages of EMU-182 (77% mfl) and EMU-235 (100% mfl). The delayed fusion of the hindlimb is generally consistent with what is reported for other paleognaths, although the absolute timing relative to skeletal maturity may vary (Turvey & Holdaway, 2005). The astragalus and calcaneum are the only elements that definitively fuse for *Troodon.* Fusion of the astragalus and calcaneum is commonly reported for troodontids, especially in specimens displaying other features of maturity (Lee et al., 2023). It is important to note that the holotype specimen for the troodontid *Almas ukhaa* exhibits fusion of these two elements, despite having a suite of immature characters (Pei et al., 2017). It is possible that MOR 748 (100% mfl) has a fused tarsometatarsus, but poor preservation precludes a definitive interpretation. Appendicular fusion that is not confidently observed in the *Troodon* sample is variably reported for other troodontids. This includes fusion of the scapulocoracoid (Gao et al., 2012), tibiotarsus (Cau & Madzia, 2021; Shen et al., 2017; Xu et al., 2012), distal tarsals (Norell et al., 2009; Xu et al., 2012), metatarsus (Xu et al., 2012), and pelvic elements (Norell et al., 2009; van der Reest & Currie, 2017). The absence of these features in the *Troodon* sample suggests that such fusion events happen relatively late in ontogeny, if at all.

It is possible that the more extensive appendicular fusion in the emu reflects peramorphic evolution among paravian dinosaurs, as has been suggested for other aspects of appendicular evolution in this clade (Griffin et al., 2022). However, pelvic fusion has been suggested to be highly convergent among maniraptorans (Wang et al., 2017). Additionally, the pattern and timing of appendicular fusion can be variable even among closely related archosaurs (Brochu, 1995). Just outside of Paraves, for example, extensive appendicular fusion that approaches the extremes observed in the emu has been reported in members of Oviraptorosauria (Funston et al., 2016). Furthermore, the timing of appendicular fusion events in some oviraptorosaurs, such as the fusion of the tarsometatarsus in immature individuals (Funston et al., 2019), is distinct from what is observed in the emu and *Troodon*.

### Utility of Skeletal Fusion in Ontogenetic Interpretations

The unique patterns of postcranial fusion in the emu and *Troodon* highlight the issue of using distantly related taxa to guide the ontogenetic interpretations of fossil specimens. This suggestion is consistent with Griffin et al. (2021), which reviews the high degree of variation in skeletal fusion patterns among different reptile groups. Given this high amount of variation

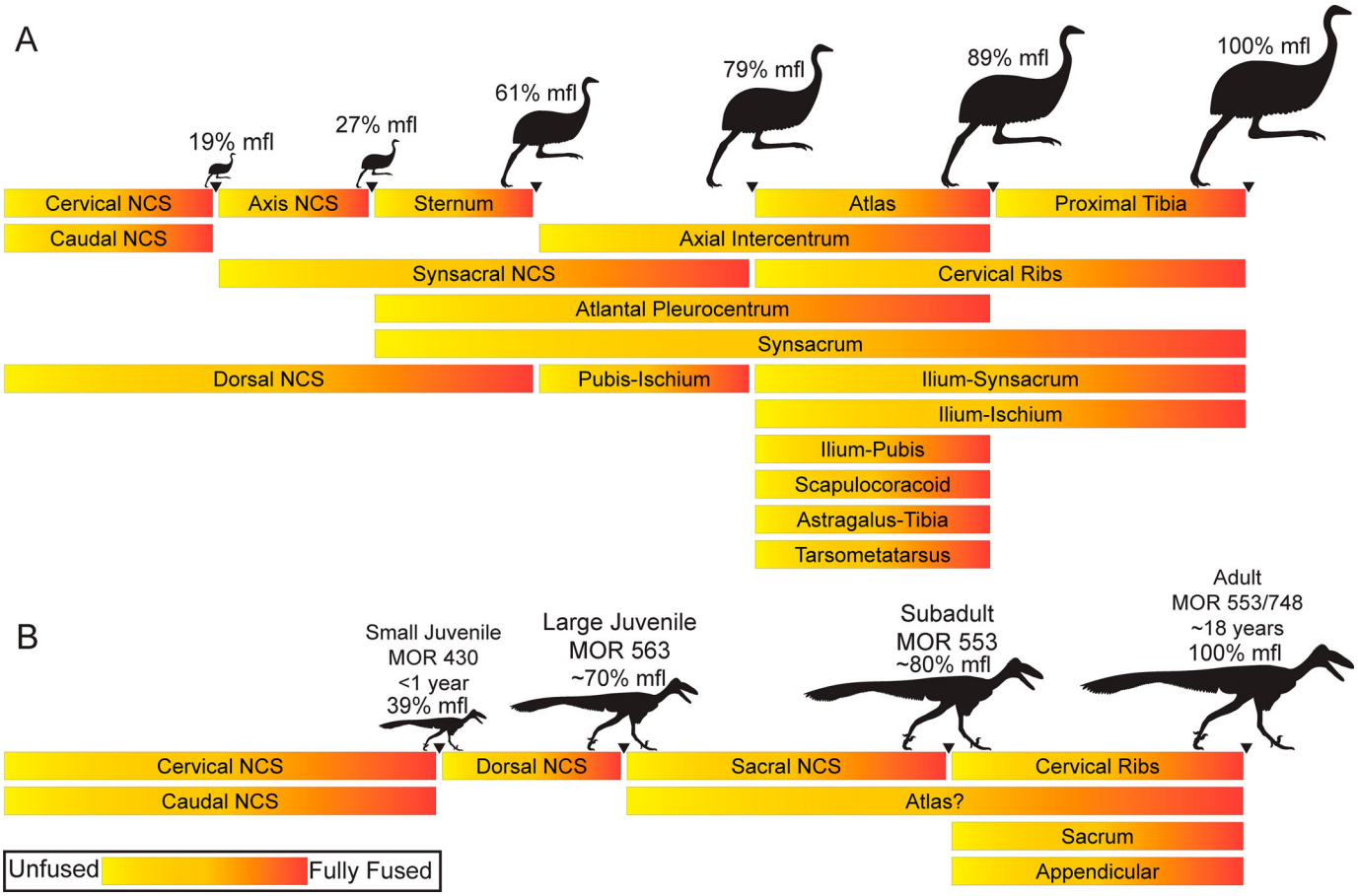


FIGURE 14. Summary figure of postcranial fusion events for the **A**, emu, and **B**, *Troodon*. **Abbreviations**: **mfl**, maximum femur length; **NCS**, neurocentral suture. *Troodon* made with reference to work by Scott Hartman (https://creativecommons.org/licenses/by-nc-sa/3.0/).

among archosaurs and reptiles as a whole, it is possible that the similarities between the emu and *Troodon* are purely homoplastic. While Griffin and Nesbitt (2016) suggest that ontogenetic polymorphism for archosaurs is less extreme for taxa more closely related to crown birds, this study does not intensively explore interspecific variations in ontogeny. However, this shared pattern of fusion between these two taxa is not necessarily meaningless, even if it is the result of convergent evolution. As has been argued for other taxa, these similarities could be the result of shared biomechanical stresses between the emu and *Troodon* (e.g., James, 2009; Gambaryan et al., 2005; Mulder, 2001; VanBuren & Evans, 2016). If the biomechanical properties of an organism do influence the pattern of skeletal fusion, then such characteristics must be considered in addition to phylogenetic information before using skeletal fusion for an ontogenetic assessment.

A more holistic investigation of skeletal fusion patterns throughout the entirety of Archosauria is needed before the data reported here and by other researchers (e.g., Brochu, 1996; Irmis, 2007) can be confidently applied to the study of other taxa. This includes intensive sampling across the clade to not only document the phylogenetic variation of skeletal fusion characters but also identify the functional drivers of this diversity (e.g., adaptations for locomotion or large body size). Doing so will allow for a more nuanced understanding of the evolution of archosaur growth and provide a detailed framework for accurately assessing the maturity of fossil archosaur specimens.

## CONCLUSION

The patterns of neurocentral suture closure in the emu (*Dromaius novaehollandiae*) and *Troodon formosus* contrast with what is observed in crocodilians, neognath birds, and other theropod groups. Unlike crocodilians and some neognaths, neurocentral suture closure appears to originate cranially and caudally and converges in the sacral region early in ontogeny for both emus and *Troodon*. Fusion of the atlas, axis, cervical ribs, sacrum/synsacrum, and appendicular elements are all events that happen late in ontogeny for both the emu and *Troodon*, although appendicular fusion is not as extensive in the latter taxon. Delayed fusion of the atlas and axis are widespread throughout Archosauria and are potentially reliable indicators of maturity for this group. This study not only provides additional data on paravian dinosaur ontogeny but also emphasizes the need for a more holistic understanding of fusion patterns among vertebrate groups before precise ontogenetic interpretations can be made with this information.

## ACKNOWLEDGMENTS

We thank H. Boekenheide and Z. Hannebaum with the Varricchio Family Paleontology Laboratory for providing the space and resources for specimen preparation; C. Ancell, T. Babcock, B. Clark, Z. Cooper, H. Finch, D. Johnson, G. Lafaye, and K. Tucker for assistance with specimen preparation; the Blackfeet Nation and Montana Emu Ranch for specimen donation; J. Scannella and E. Metz at MOR for specimen access and for

taking action to prevent a dermestid beetle infestation in the paleontology collections; the reviewers and editors of this manuscript; R. and V. Caldwell for their support of our pungent emu endeavors; Montana State University Undergraduate Scholars Program for funding; and C. Griffin, the anonymous reviewer, and the journal editors for providing helpful feedback with this manuscript.

## AUTHOR CONTRIBUTIONS

DJV generated the project idea. HRC and EB facilitated specimen preparation. All authors were involved in data collection. HRC analyzed the data and wrote the manuscript. HRC and DJV edited the manuscript.

## DATA AVAILABILITY STATEMENT

The authors confirm that the data supporting the findings of this study are available within the article and its supplementary materials. Supplementary files are available on Morphobank through the following link.: http://morphobank.org/permalink/?P5883

## DISCLOSURE STATEMENT

No potential conflict of interest was reported by the author(s).

## ORCID

Heath R. Caldwell http://orcid.org/0009-0003-8415-8541
David J. Varricchio http://orcid.org/0000-0002-0594-0929

## SUPPLEMENTARY FILES

Supplementary _File_1.nex: character matrix used for emu dataset with brief character descriptions.

Supplementary_File_2.nex: character matrix used for *Troodon* dataset with brief character descriptions.

Supplementary_File_3.tre: most parsimonious ontogenetic tree resolved for emu dataset.

Supplementary_File_4.tre: most parsimonious ontogenetic tree resolved for *Troodon* dataset.

## LITERATURE CITED

Agnolin, F. L., Motta, M. J., Brissón Egli, F., Lo Coco, G., & Novas, F. E. (2019). Paravian phylogeny and the dinosaur-bird transition: an overview. *Frontiers in Earth Science*, *6*, 252. https://doi.org/10.3389/feart.2018.00252

Averianov, A., Skutschas, P., & Lopatin, A. (2023). Ontogeny and miniaturization of Alvarezsauridae (Dinosauria, Theropoda). *Biological Communications*, *68*(2), 65–73. doi:10.21638/spbu03.2023.201

Bailleul, A. M., Scannella, J. B., Horner, J. R., & Evans, D. C. (2016). Fusion patterns in the skulls of modern archosaurs reveal that sutures are ambiguous maturity indicators for the Dinosauria. *PLoS ONE*, *11*(2), e0147687. https://doi.org/10.1371/journal.pone.0147687

Bever, G. S., & Norell, M. A. (2009). The perinate skull of *Byronosaurus* (Troodontidae) with observations on the cranial ontogeny of paravian theropods. *American Museum Novitates*, *2009*(3657), 1–52. https://doi.org/10.1206/650.1

Boekenheide, H. R. (2023). The hind limb ontogeny of *Troodon formosus* (Master's thesis, Montana State University-Bozeman, College of Letters & Science). https://scholarworks.montana.edu/handle/1/17939.

Brochu, C. A. (1995). Heterochrony in the crocodylian scapulocoracoid. *Journal of Herpetology*, *29*(3), 464–468. https://doi.org/10.2307/1565002

Brochu, C. A. (1996). Closure of neurocentral sutures during crocodilian ontogeny: implications for maturity assessment in fossil archosaurs. *Journal of Vertebrate Paleontology*, *16*(1), 49–62. https://doi.org/10.1080/02724634.1996.10011283

Cau, A., & Madzia, D. (2021). The phylogenetic affinities and morphological peculiarities of the bird-like dinosaur *Borogovia gracilicrus* from the Upper Cretaceous of Mongolia. *PeerJ*, *9*, e12640. doi:10.7717/peerj.12640

Campione, N. E., Evans, D. C., Brown, C. M., & Carrano, M. T. (2014). Body mass estimation in non-avian bipeds using a theoretical conversion to quadruped stylopodial proportions. *Methods in Ecology and Evolution*, *5*(9), 913–923. https://doi.org/10.1111/2041-210X.12226

Carrano, M. T., Sampson, S. D., & Forster, C. A. (2002). The osteology of *Masiakasaurus knopfleri*, a small abelisauroid (Dinosauria: Theropoda) from the Late Cretaceous of Madagascar. *Journal of Vertebrate Paleontology*, *22*(3), 510–534. https://doi.org/10.1671/0272-4634(2002)022[0510:TOOMKA]2.0.CO;2

Castanet, J., Curry Rogers, K., Cubo, J., & Jacques-Boisard, J. (2000). Periosteal bone growth rates in extant ratites (ostriche and emu). Implications for assessing growth in dinosaurs. *Comptes Rendus de l'Académie des Sciences - Series III - Sciences de la Vie*, *323*(6), 543–550. https://doi.org/10.1016/S0764-4469(00)00181-5

Cubo, J., Le Roy, N., Martinez-Maza, C., & Montes, L. (2012). Paleohistological estimation of bone growth rate in extinct archosaurs. *Paleobiology*, *38*(2), 335–349. https://doi.org/10.1666/08093.1

Currie, P. J. (1987). Bird-like characteristics of the jaws and teeth of troodontid theropods Dinosauria, Saurischia). *Journal of Vertebrate Paleontology*, *7*(1), 72–81. https://doi.org/10.1080/02724634.1987.10011638

Currie, P. J., & Peng, J. H. (1993). A juvenile specimen of *Saurornithoides mongoliensis* from the Upper Cretaceous of northern China. *Canadian Journal of Earth Sciences*, *30*(10), 2224–2230. https://doi.org/10.1139/e93-193

D'Emic, M. D., O'Connor, P. M., Sombathy, R. S., Cerda, I., Pascucci, T. R., Varricchio, D. J., Pol, D., Dave, A., Coria, R. A., & Curry Rogers, K. A. (2023). Developmental strategies underlying gigantism and miniaturization in non-avialan theropod dinosaurs. *Science*, *379*(6634), 811–814. https://doi.org/10.1126/science.adc8714

Dodson, P. (1975). Taxonomic implications of relative growth in lambeosaurine hadrosaurs. *Systematic Biology*, *24*(1), 37–54. https://doi.org/10.1093/sysbio/24.1.37

Erickson, G. M., Curry Rogers, K., Varricchio, D. J., Norell, M. A., & Xu, X. (2007). Growth patterns in brooding dinosaurs reveals the timing of sexual maturity in non-avian dinosaurs and genesis of the avian condition. *Biology Letters*, *3*(5), 558–561. https://doi.org/10.1098/rsbl.2007.0254

Funston, G. F. (2024). Osteology of the two-fingered oviraptorid *Oksoko avarsan* (Theropoda: Oviraptorosauria). *Zoological Journal of the Linnean Society*, zlae011. https://doi.org/10.1093/zoolinnean/zlae011

Funston, G. F., Currie, P. J., Eberth, D. A., Ryan, M. J., Chinzorig, T., Badamgarav, D., & Longrich, N. R. (2016). The first oviraptorosaur (Dinosauria: Theropoda) bonebed: evidence of gregarious behaviour in a maniraptoran theropod. *Scientific Reports*, *6*(1), 35782. https://doi.org/10.1038/srep35782

Funston, G. F., Currie, P. J., Ryan, M. J., & Dong, Z. M. (2019). Birdlike growth and mixed-age flocks in avimimids (Theropoda, Oviraptorosauria). *Scientific Reports*, *9*(1), 18816. https://doi.org/10.1038/s41598-019-55038-5

Gambaryan, P. P., Zherebtsova, O. V., & Platonov, V. V. (2005). Morphofunctional analysis of the cervical-thoracic region in some burrowing mammals. *Russian Journal of Theriology*, *4*(1), 13–41. doi:10.15298/rusjtheriol.04.1.02

Gao, C., Morschhauser, E. M., Varricchio, D. J., Liu, J., & Zhao, B. (2012). A second soundly sleeping dragon: new anatomical details of the Chinese troodontid *Mei long* with implications for phylogeny and taphonomy. https://doi.org/10.1371/journal.pone.0045203

Gauthier, J. (1986). Saurischian monophyly and the origin of birds. *Memoirs of the California Academy of sciences*, *8*, 1–55.

Goloboff, P. A., & Morales, M. E. (2023). TNT version 1.6, with a graphical interface for MacOS and Linux, including new routines in parallel. *Cladistics*, *39*(2), 144–153. https://doi.org/10.1111/cla.12524

Goonewardene, L. A., Wang, Z., Okine, E., Zuidhof, M. J., Dunk, E., & Onderka, D. (2003). Comparative growth characteristics of emus (*Dromaius novaehollandiae*). *Journal of Applied Poultry Research*, *12*(1), 27–31. https://doi.org/10.1093/japr/12.1.27

Griffin, C. T. (2018). Developmental patterns and variation among early theropods. *Journal of Anatomy*, *232*(4), 604–640. https://doi.org/10.1111/joa.12775

Griffin, C. T., Botelho, J. F., Hanson, M., Fabbri, M., Smith-Paredes, D., Carney, R. M., Norell, M. A., Egawa, S., Gatesy, S. M., Rowe, T. B., Elsey, R. M., Nesbitt, S. J., & Bhullar, B. A. S. (2022). The developing bird pelvis passes through ancestral dinosaurian conditions. *Nature*, *608*(7922), 346–352. https://doi.org/10.1038/s41586-022-04982-w

Griffin, C. T., & Nesbitt, S. J. (2016). Anomalously high variation in postnatal development is ancestral for dinosaurs but lost in birds. *Proceedings of the National Academy of Sciences*, *113*(51), 14757–14762. https://doi.org/10.1073/pnas.1613813113

Griffin, C. T., Stocker, M. R., Colleary, C., Stefanic, C. M., Lessner, E. J., Riegler, M., Formoso, K., Koeller, K., & Nesbitt, S. J. (2021). Assessing ontogenetic maturity in extinct saurian reptiles. *Biological Reviews*, *96*(2), 470–525. https://doi.org/10.1111/brv.12666

Heinrich, C., Paes Neto, V. D., Lacerda, M. B., Martinelli, A. G., Fiedler, M. S., & Schultz, C. L. (2021). The ontogenetic pattern of neurocentral suture closure in the axial skeleton of Hyperodapedontinae (Archosauromorpha, Rhynchosauria) and its evolutionary implications. *Palaeontology*, *64*(3), 409–427. https://doi.org/10.1111/pala.12528

Herring, S. W. (2008). Mechanical influences on suture development and patency. *Craniofacial sutures*, *12*, 41–56. https://doi.org/10.1159/000115031

Hone, D. W., Farke, A. A., & Wedel, M. J. (2016). Ontogeny and the fossil record: what, if anything, is an adult dinosaur? *Biology letters*, *12*(2), 20150947. https://doi.org/10.1098/rsbl.2015.0947

Irmis, R. B. (2007). Axial skeleton ontogeny in the Parasuchia (Archosauria: Pseudosuchia) and its implications for ontogenetic determination in archosaurs. *Journal of Vertebrate Paleontology*, *27*(2), 350–361. https://doi.org/10.1671/0272-4634(2007)27[350:ASOITP]2.0.CO;2

James, H. F. (2009). Repeated evolution of fused thoracic vertebrae in songbirds. *The Auk*, *126*(4), 862–872. https://doi.org/10.1525/auk.2009.08194

Lee, S., Lee, Y. N., Park, J. Y., Kim, S. H., Badamkhatan, Z., Idersaikhan, D., & Tsogtbaatar, K. (2023). The first troodontid (Dinosauria: Theropoda) from the Upper Cretaceous Baruungoyot Formation of Mongolia. *Journal of Vertebrate Paleontology*, e2364746. https://doi.org/10.1080/02724634.2024.2364746

Longrich, N. R., & Currie, P. J. (2009). A microraptorine (Dinosauria–Dromaeosauridae) from the late Cretaceous of North America. *Proceedings of the National Academy of Sciences*, *106*(13), 5002–5007. https://doi.org/10.1073/pnas.0811664106

Longrich, N. R., & Saitta, E. T. (2024). Taxonomic status of *Nanotyrannus lancensis* (Dinosauria: Tyrannosauroidea)—a distinct taxon of small-bodied tyrannosaur. *Fossil Studies*, *2*(1), 1–65. https://doi.org/10.3390/fossils2010001

Malafaia, E., Mocho, P., Escaso, F., & Ortega, F. (2017). A juvenile allosauroid theropod (Dinosauria, Saurischia) from the Upper Jurassic of Portugal. *Historical Biology*, *29*(5), 654–676. https://doi.org/10.1080/08912963.2016.1231183

Maloney, S. K., & Dawson, T. J. (1993). Sexual dimorphism in basal metabolism and body temperature of a large bird, the emu. *The Condor*, 1034–1037. https://doi.org/10.2307/1369441

Marsh, A. D., & Rowe, T. B. (2020). A comprehensive anatomical and phylogenetic evaluation of *Dilophosaurus wetherilli* (Dinosauria, Theropoda) with descriptions of new specimens from the Kayenta Formation of northern Arizona. *Journal of Paleontology*, *94*(S78), 1–103. https://doi.org/10.1017/jpa.2020.14

Moro, D., Kerber, L., Müller, R. T., & Pretto, F. A. (2021). Sacral co-ossification in dinosaurs: The oldest record of fused sacral vertebrae in Dinosauria and the diversity of sacral co- ossification patterns in the group. *Journal of Anatomy*, *238*(4), 828–844. https://doi.org/10.1111/joa.13356

Mulder, E. W. (2001). Co-ossified vertebrae of mosasaurs and cetaceans: implications for the mode of locomotion of extinct marine reptiles. *Paleobiology*, *27*(4), 724–734. https://doi.org/10.1666/0094-8373(2001)027<0724:COVOMA>2.0.CO;2

Naish, D., & Sweetman, S. C. (2011). A tiny maniraptoran dinosaur in the Lower Cretaceous Hastings Group: evidence from a new vertebrate-bearing locality in south-east England. *Cretaceous Research*, *32*(4), 464–471. https://doi.org/10.1016/j.cretres.2011.03.001

Nesbitt, S. J., Denton Jr, R. K., Loewen, M. A., Brusatte, S. L., Smith, N. D., Turner, A. H., Kirkland, J. I., McDonald, A. T., & Wolfe, D. G. (2019). A mid-Cretaceous tyrannosauroid and the origin of North American end-Cretaceous dinosaur assemblages. *Nature Ecology & Evolution*, *3*(6), 892–899. https://doi.org/10.1038/s41559-019-0888-0

Norell, M. A., Clark, J. M., & Chiappe, L. M. (2001). An embryonic oviraptorid (Dinosauria: Theropoda) from the upper Cretaceous of Mongolia. *American Museum Novitates*, *2001*(3315), 1–20. https://doi.org/10.1206/0003-0082(2001)315<0001:AEODTF>2.0.CO;2

Norell, M. A., Clark, J. M., Turner, A. H., Makovicky, P. J., Barsbold, R., & Rowe, T. (2006). A new dromaeosaurid theropod from Ukhaa Tolgod (Ömnögov, Mongolia). *American Museum Novitates*, *2006*(3545), 1–51. https://doi.org/10.1206/0003-0082(2006)3545[1:ANDTFU]2.0.CO;2

Norell, M. A., Makovicky, P. J., Bever, G. S., Balanoff, A. M., Clark, J. M., Barsbold, R., & Rowe, T. (2009). A review of the Mongolian cretaceous dinosaur *Saurornithoides* (Troodontidae:: Theropoda). *American Museum Novitates*, *2009*(3654), 1–63. https://doi.org/10.1206/648.1

O'Connor, P. M. (2007). The postcranial axial skeleton of *Majungasaurus crenatissimus* (Theropoda: Abelisauridae) from the Late Cretaceous of Madagascar. *Journal of Vertebrate Paleontology*, *27*(S2), 127–163. https://doi.org/10.1671/0272-4634(2007)27[127:TPASOM]2.0.CO;2

Pei, R., Norell, M. A., Barta, D. E., Bever, G. S., Pittman, M., & Xu, X. (2017). Osteology of a new late Cretaceous troodontid specimen from Ukhaa Tolgod, Ömnögovi Aimag, Mongolia. *American Museum Novitates*, *2017*(3889), 1–47. https://doi.org/10.1206/3889.1

Poust, A. W., Gao, C., Varricchio, D. J., Wu, J., & Zhang, F. (2020). A new microraptorine theropod from the Jehol Biota and growth in early dromaeosaurids. *The Anatomical Record*, *303*(4), 963–987. https://doi.org/10.1002/ar.24343

Senter, P., Kirkland, J. I., DeBlieux, D. D., Madsen, S., & Toth, N. (2012). New dromaeosaurids (Dinosauria: Theropoda) from the Lower Cretaceous of Utah, and the evolution of the dromaeosaurid tail. *PLoS ONE*, *7*(5), e36790. https://doi.org/10.1371/journal.pone.0036790

Shen, C., Zhao, B., Gao, C., Lü, J., Kundrát, M., & H, G. A. O. (2017). A new troodontid dinosaur (*Liaoningvenator curriei* gen. et sp. nov.) from the early cretaceous Yixian Formation of Western Liaoning Province, China. *Acta Geologica Sinica - English Edition*, *91*(3), 763–780. doi:10.1111/1755-6724.13307

Smith, N. D., Makovicky, P. J., Hammer, W. R., & Currie, P. J. (2007). Osteology of *Cryolophosaurus ellioti* (Dinosauria: Theropoda) from the Early Jurassic of Antarctica and implications for early theropod evolution. *Zoological Journal of the Linnean Society*, *151*(2), 377–421. https://doi.org/10.1111/j.1096-3642.2007.00325.x

Starck, J. M. (1993). Evolution of avian ontogenies. *Current Ornithology*, *10*, 275–366. https://doi.org/10.1007/978-1-4615-9582-3_6

Sues, H. D. (1997). On *Chirostenotes*, a Late Cretaceous oviraptorosaur (Dinosauria: Theropoda) from western North America. *Journal of vertebrate Paleontology*, *17*(4), 698–716. https://doi.org/10.1080/02724634.1997.10011018

Turvey, S. T., & Holdaway, R. N. (2005). Postnatal ontogeny, population structure, and extinction of the giant moa *Dinornis*. *Journal of Morphology*, *265*(1), 70–86. https://doi.org/10.1002/jmor.10341

Tsuihiji, T., Barsbold, R., Watabe, M., Tsogtbaatar, K., Chinzorig, T., Fujiyama, Y., & Suzuki, S. (2014). An exquisitely preserved troodontid theropod with new information on the palatal structure from the Upper Cretaceous of Mongolia. *Naturwissenschaften*, *101*(2), 131–142. https://doi.org/10.1007/s00114-014-1143-9

VanBuren, C. S., & Evans, D. C. (2016). Evolution and function of anterior cervical vertebral fusion in tetrapods. *Biological Reviews*, *92*(1), 608–626. https://doi.org/10.1111/brv.12245

van der Reest, A. J., & Currie, P. J. (2017). Troodontids (Theropoda) from the Dinosaur Park Formation, Alberta, with a description of a unique new taxon: implications for deinonychosaur diversity in North America. *Canadian Journal of Earth Sciences*, *54*(9), 919–935. https://doi.org/10.1139/cjes-2017-0031

Varricchio, D. J. (1993). Bone microstructure of the Upper Cretaceous theropod dinosaur *Troodon formosus*. *Journal of Vertebrate Paleontology*, *13*(1), 99–104. https://doi.org/10.1080/02724634.1993.10011490

Varricchio, D. J. (1995). Taphonomy of Jack's Birthday Site, a diverse dinosaur bonebed from the Upper Cretaceous Two Medicine Formation of Montana. *Palaeogeography, Palaeoclimatology, Palaeoecology*, *114*(2–4), 297–323. https://doi.org/10.1016/0031-0182(94)00084-L

Varricchio, D. J., Horner, J. R., & Jackson, F. D. (2002). Embryos and eggs for the Cretaceous theropod dinosaur *Troodon formosus*. *Journal of Vertebrate Paleontology*, *22*(3), 564–576. https://doi.org/10.1671/0272-4634(2002)022[0564:EAEFTC]2.0.CO;2

Varricchio, D. J., Hogan, J. D., & Gardner, J. D. (in press). Troodontid specimens from the Cretaceous Two Medicine Formation of Montana (USA) and the validity of *Troodon formosus*. *Journal of Paleontology*.

Varricchio, D. J., Jackson, F., Borkowski, J. J., & Horner, J. R. (1997). Nest and egg clutches of the dinosaur *Troodon formosus* and the evolution of avian reproductive traits. *Nature*, *385*(6613), 247–250. https://doi.org/10.1038/385247a0

Varricchio, D. J., Kundrát, M., & Hogan, J. (2018). An intermediate incubation period and primitive brooding in a theropod dinosaur. *Scientific Reports*, *8*(1), 12454. https://doi.org/10.1038/s41598-018-30085-6

Varricchio, D. J., Moore, J. R., Erickson, G. M., Norell, M. A., Jackson, F. D., & Borkowski, J. J. (2008). Avian paternal care had dinosaur origin. *Science*, *322*(5909), 1826–1828. doi:10.1126/science.1163245

Verrière, A., Fröbisch, N. B., & Fröbisch, J. (2022). Regionalization, constraints, and the ancestral ossification patterns in the vertebral column of amniotes. *Scientific Reports*, *12*(1), 22257. https://doi.org/10.1038/s41598-022-24983-z

Wang, M., Li, Z., & Zhou, Z. (2017). Insight into the growth pattern and bone fusion of basal birds from an Early Cretaceous enantiornithine bird. *Proceedings of the National Academy of Sciences*, *114*(43), 11470–11475. https://doi.org/10.1073/pnas.1707237114

Wang, R., & Pei, R. (2024). The smallest known specimen of *Microraptor* (Dinosauria: Dromaeosauridae) from the Jiufotang Formation in northeastern China. *Historical Biology*, doi:10.1080/08912963.2024.2385604

Wang, S., Zhang, Q., Tan, Q., Jiangzuo, Q., Zhang, H., & Tan, L. (2022). New troodontid theropod specimen from Inner Mongolia, China clarifies phylogenetic relationships of later-diverging small-bodied troodontids and paravian body size evolution. *Cladistics*, *38*(1), 59–82. https://doi.org/10.1111/cla.12467

Woodward, H. N., Tremaine, K., Williams, S. A., Zanno, L. E., Horner, J. R., & Myhrvold, N. (2020). Growing up *Tyrannosaurus rex*: Osteohistology refutes the pygmy "*Nanotyrannus*" and supports ontogenetic niche partitioning in juvenile *Tyrannosaurus*. *Science Advances*, *6*(1), eaax6250. https://doi.org/10.1126/sciadv.aax6250

Xu, X., & Norell, M. A. (2004). A new troodontid dinosaur from China with avian-like sleeping posture. *Nature*, *431*(7010), 838–841. https://doi.org/10.1038/nature02898

Xu, X., & Xiaolin, W. (2004). A new troodontid (Theropoda: Troodontidae) from the Lower Cretaceous Yixian formation of western Liaoning, China. *Acta Geologica Sinica - English Edition*, *78*(1), 22–26. https://doi.org/10.1111/j.1755-6724.2004.tb00671.x

Xu, X., Zhao, Q., Sullivan, C., Tan, Q. W., Sander, M., & Ma, Q. Y. (2012). The taxonomy of the troodontid IVPP V 10597 reconsidered. *Vertebrata PalAsiatica*, *50*, 140–150.

Yates, A. M., & Kitching, J. W. (2003). The earliest known sauropod dinosaur and the first steps towards sauropod locomotion. *Proceedings of the Royal Society of London. Series B: Biological Sciences*, *270*(1525), 1753–1758. https://doi.org/10.1098/rspb.2003.2417

Zanno, L. E. (2010). Osteology of *Falcarius utahensis* (Dinosauria: Theropoda): characterizing the anatomy of basal therizinosaurs. *Zoological Journal of the Linnean Society*, *158*(1), 196–230. https://doi.org/10.1111/j.1096-3642.2009.00464.x

Handling Editor: Gabriel Bever.
Phylogenetics Editor: Pedro Godoy.